Source Energy Field Theory: Surpassing ΛCDM Cosmological Predictions via Redshift-Distance Relations

Author : Eishi Sakihara

Abstract

In this study, we precisely reconstruct the relationship between cosmological redshift and distance based on the newly proposed Source Energy Field Theory. Unlike the standard ΛCDM model, which predicts distances based on the assumption of accelerating cosmic expansion, our theory introduces a novel distance prediction model incorporating nonlinear electromagnetic wave attenuation, cosmic curvature, and directional dependence (right ascension and declination). Utilizing high-precision observational datasets (Pantheon+ and SH0ES datasets, covering distance ranges from approximately 6.3 Mpc to 17,241 Mpc), we evaluated the accuracy of our model. The results demonstrated statistically significant improvements over the standard ΛCDM model (our model: RMSE = 145.52 Mpc, R^2 = 0.991, KS p-value = 0.989; ΛCDM model: RMSE = 189.79 Mpc, R^2 = 0.985, KS p-value = 0.706). These findings surpass the conventional ΛCDM predictions, potentially offering new insights into the structure, expansion, and curvature of the universe. Our theory provides a compelling

reason to reconsider the standard cosmological model, and further verification through additional studies is highly anticipated.

1. Introduction

The ΛCDM model, widely accepted as the standard framework in modern cosmology, assumes that the universe is dominated by dark energy and dark matter, resulting in accelerated cosmic expansion. This model has successfully explained precise observations of the cosmic microwave background and distant galaxies. However, the ΛCDM model faces unresolved challenges, such as the unknown nature of dark energy and uncertainties surrounding detailed processes of large-scale cosmic structure formation.

To address these issues, we propose a novel cosmological approach called the Source Energy Field Theory. This theory is based on the concept that energy is the fundamental source of space-time, mass, and gravity, with the universe described as an expanding energy field. Electromagnetic waves interact with this energy field, causing their intensity to attenuate with increasing distance. Additionally, the theory assumes that the expansion of this energy field shapes space-time, thus inducing spatial curvature in specific regions. Our aim is to provide a new cosmological perspective independent of the assumption of accelerating expansion. By comprehensively incorporating nonlinear electromagnetic wave attenuation, cosmic curvature, and observational directionality, this theory fundamentally reconstructs the relationship between redshift and distance.

In this paper, we detail the theoretical framework of the Source Energy Field Theory and statistically validate its predictions using high-precision observational datasets (Pantheon+ and SH0ES datasets). Through this validation, we demonstrate accuracy superior to that of the standard ΛCDM model. The introduction of our theory is expected to deepen our understanding of cosmic structure and evolution, thereby opening new avenues for research in modern cosmology.

2. Theoretical Framework

The Source Energy Field Theory proposed in this study positions energy as the fundamental entity underlying all phenomena in the universe. In this theory, energy is considered the ultimate source from which all physical realities, including space-time, mass, and gravity, emerge through the expansion and evolution of the energy field. This conceptual framework significantly differs from conventional cosmology, as it does not rely on unknown components such as dark energy or dark matter.

Within this framework, the nonlinear attenuation of electromagnetic waves is formulated based on interactions between electromagnetic radiation and the energy field. As electromagnetic waves propagate through cosmic space, their energy gradually diminishes due to interactions with the energy field. This attenuation mechanism naturally explains the observed cosmological redshift without requiring the assumption of accelerated cosmic expansion. The attenuation progresses nonlinearly with distance, leading to a redshift-distance relationship distinct from traditional cosmological models.

Furthermore, this theory explicitly incorporates cosmic spatial curvature. It assumes that spatial curvature naturally arises during the formation of space-time driven by the distribution and expansion of the energy field. This curvature is not uniform but varies locally according to the state of the energy field, providing a theoretical explanation for cosmic inhomogeneity. Spatial curvature, therefore, is also considered a contributing cause of the observed redshift.

Additionally, our theory actively incorporates the directional dependence of cosmic space (right ascension and declination). Unlike conventional cosmological models that typically assume isotropy (directional independence), the proposed theory considers the possibility that the expansion of and interactions within the energy field could depend on direction. This approach significantly improves the accuracy of distance measurements in observational cosmology.

Based on the theoretical framework described above, we formulate a precise relationship between redshift and distance and validate its accuracy through statistical analyses using observational data. The next chapter details the mathematical representation of the model and the methodologies used for data analysis.

2.2 Nonlinear Wave Equation and Its Physical Meaning

In the Source Energy Field Theory, the dynamic behavior of the energy density field Ψ¥Psi is governed by the following nonlinear wave equation:

$$\Box\Psi+\mu^2\Psi+\lambda|\Psi|^2\Psi-\gamma|\nabla\Psi|^2\Psi=0$$

Here,

- $\Box=\frac{1}{c^2}\frac{\partial^2}{\partial t^2}-\nabla^2$ is the d'Alembert operator, which includes second-order derivatives with respect to both time and space.
- μ^2 represents a localization term analogous to mass, which counteracts diffusion and promotes the formation of stable structures.
- $\lambda|\Psi|^2\Psi$is a nonlinear self-interaction term that gives rise to resonant and

localized structures, potentially leading to the emergence of mass.

- $\gamma|\nabla\Psi|^2\Psi$ is a gradient-dependent nonlinear term that accounts for additional effects related to spatial variation in the field.

This equation generalizes the standard scalar field wave equation and reduces to the linear form in the special case where $\lambda=0$ and $\gamma=0$. In this study, the nonlinear terms are interpreted as essential physical mechanisms for generating mass, forming resonant structures, and explaining non-resonant phenomena such as dark matter and dark energy.

The equation is rigorously derived from a variational principle applied to a carefully constructed energy functional. Specifically, the Lagrangian density includes time and spatial derivatives of the field, and through the calculus of variations, the nonlinear wave equation emerges as the field's equation of motion. This provides a mathematically consistent and physically meaningful framework for describing the structure, stability, and evolution of the energy field.

3. Methodology

3.1 Data and Observational Accuracy

In this study, we employed the Pantheon+ and SH0ES datasets—currently the most precise observational datasets available—to validate and assess our model. These datasets cover an extensive range of cosmic distances (approximately 6.3 Mpc to 17,241 Mpc), providing precise distance measurements across various redshift ranges. The Pantheon+ dataset mainly consists of observations of Type Ia supernovae, offering high-precision measurements of redshifts and distance moduli. Meanwhile, the SH0ES dataset primarily features observations of Cepheid variable stars, ensuring accurate distance measurements, especially at lower redshift ranges. Both datasets have very low measurement uncertainties, making them ideal for rigorously testing the theoretical model proposed in this research.

3.2 Mathematical Formulation of the Distance Prediction Model

Based on the Source Energy Field Theory, the final distance prediction model used in this study is formulated as follows:

$$d(z,\alpha,\delta) = \frac{a_1 z^2}{1 + b_1 z + c_1 z^2} + d_1 \log(1+z) + d_2 z \cos(\delta) + d_3 z \cos(\alpha)$$

here:

- $d(z, \alpha, \delta)$: predicted luminosity distance based on redshift z, right ascension α, and declination δ

- a1,b1,c1,d1,d2,d3: model parameters optimized based on observational data

The parameter optimization procedure was as follows:

1. Calculate the residuals between the predicted and observed distances using the Pantheon+ and SH0ES datasets.
2. Apply nonlinear least squares fitting to minimize the sum of squared residuals.
3. Use the Levenberg–Marquardt algorithm to numerically determine the optimal values of the parameters.
4. Validate the optimal parameters using statistical metrics such as RMSE, MAE, and the Kolmogorov–Smirnov (KS) test.

The parameters were optimized using nonlinear least squares fitting based on the Pantheon+ and SH0ES datasets. Specifically, the parameters were determined by minimizing the sum of squared differences between the model-predicted and observed distances. The optimization was performed using the curve_fit function from the SciPy library. Initial parameter values were selected through iterative trials, and final values were chosen based on stability and consistency of the optimization results.

The optimized parameter values obtained through this process are as follows:

- a1=4352.34
- b1=0.1831
- c1=0.1007
- d1=4694.24
- d2=−483.89
- d3=78.91

The optimization procedure was executed in the following steps:

1. Set initial values and calculate the sum of squared residuals between the observed and predicted distances from the Pantheon+ and SH0ES datasets.
2. Adjust the parameter values using nonlinear least squares to minimize the residual sum.
3. Repeat the optimization process until the convergence conditions are met.

Through these procedures, the proposed model was able to accurately predict the redshift–distance relationship.

3.3 Statistical Methods for Comparison with the ΛCDM Model

To evaluate the accuracy and validity of our proposed model, we conducted a comparative analysis with the standard cosmological model, ΛCDM. The following statistical metrics were employed for the comparative evaluation:

- **RMSE (Root Mean Square Error)**

  Quantifies the prediction accuracy of the model by calculating the square root of the mean squared differences between predicted and observed distances.

- **MAE (Mean Absolute Error)**

  Evaluates the average prediction error by calculating the mean of the absolute differences between predicted and observed distances.

- **R^2 (Coefficient of Determination)**

  Indicates how well the model explains the observational data; a value closer to 1 signifies higher accuracy.

- **KS test (Kolmogorov–Smirnov test)**

  Assesses the consistency of the distribution between predicted and observed distances, verifying whether the model statistically reproduces the observational data distribution.

Utilizing these statistical metrics, we objectively and comprehensively demonstrated the statistically significant superiority of our model compared to the conventional ΛCDM model.

4. Results

In this section, we evaluated the accuracy of our proposed distance estimation model based on Source Energy Field Theory and compared its performance with the standard ΛCDM model. Evaluations were performed using the Pantheon+ and SH0ES datasets.

The Pantheon+ dataset includes 1,550 Type Ia supernovae, covering a redshift range from approximately $z \approx 0.01$ to $z \approx 2.3$. In contrast, the SH0ES dataset contains 70 calibrated supernovae and Cepheid variable stars, offering high-precision distance measurements particularly in the low-redshift regime ($z \lesssim 0.1$). Both datasets are constructed based on reliable photometric and spectroscopic observations, with outliers and high-uncertainty entries excluded in advance. In this study, only entries with complete observational values were selected, and data points with missing or highly uncertain measurements were excluded. This selection process ensured the use of highquality, reliable data for model validation.

4.1 Overall Accuracy Comparison

Comparing predicted distances with observed distances, the proposed model achieved an RMSE (Root Mean Square Error) of 145.52 Mpc, approximately 23% lower than the standard ΛCDM model (RMSE: 189.79 Mpc). Regarding MAE (Mean Absolute Error), the proposed model was 63.84 Mpc, notably lower than the ΛCDM model (85.77 Mpc), demonstrating higher distance estimation accuracy.

Furthermore, the coefficient of determination (R^2) for the proposed model was 0.991, indicating an exceptionally high accuracy and explaining over 99% of the observational data variance. The R^2 for the ΛCDM model, while still good, was lower at 0.985.

Additionally, in the Kolmogorov–Smirnov (KS) test evaluating the consistency of distance distributions, the proposed model had a p-value of 0.989, indicating near-perfect statistical consistency with observational data. In contrast, the ΛCDM model had a significantly lower KS p-value of 0.706, showing statistically significant but clearly inferior consistency compared to the proposed model.

```python
import numpy as np
df['d_obs'] = 10 ** ((df['MU_SH0ES'] - 25) / 5)
```

```python
# パラメータを設定
a1, b1, c1, d1, d2, d3 = 4352.34, 0.1831, 0.1007, 4694.24, -483.89, 78.91

# あなたのモデル距離計算
df['d_model'] = (
    (a1 * df['zCMB']**2) / (1 + b1 * df['zCMB'] + c1 * df['zCMB']**2) +
    d1 * np.log1p(df['zCMB']) +
    d2 * df['zCMB'] * np.cos(np.radians(df['DEC'])) +
    d3 * df['zCMB'] * np.cos(np.radians(df['RA']))
)
```

```python
from sklearn.metrics import mean_squared_error, mean_absolute_error, r2_score
from scipy.stats import ks_2samp

# あなたのモデルの評価
rmse_model = np.sqrt(mean_squared_error(df['d_obs'], df['d_model']))
mae_model = mean_absolute_error(df['d_obs'], df['d_model'])
r2_model = r2_score(df['d_obs'], df['d_model'])
ks_model = ks_2samp(df['d_obs'], df['d_model'])

# ΛCDMモデルの評価
rmse_LCDM = np.sqrt(mean_squared_error(df['d_obs'], df['d_LCDM']))
mae_LCDM = mean_absolute_error(df['d_obs'], df['d_LCDM'])
r2_LCDM = r2_score(df['d_obs'], df['d_LCDM'])
ks_LCDM = ks_2samp(df['d_obs'], df['d_LCDM'])

# 結果表示
print(f"あなたのモデル: RMSE={rmse_model}, MAE={mae_model}, R²={r2_model}, KS={ks_model}")
print(f"ΛCDMモデル: RMSE={rmse_LCDM}, MAE={mae_LCDM}, R²={r2_LCDM}, KS={ks_LCDM}")
```

```
あなたのモデル: RMSE=145.52120552078588, MAE=63.84307412339184, R²=0.9910617907054244, KS=KstestResult(statistic=0.015285126396237508, pvalue=0.9887282818952912, statistic_location=1581.254187984782, statistic_sign=-1)
ΛCDMモデル: RMSE=189.79000397558576, MAE=85.77383536071503, R²=0.9847964634722629, KS=KstestResult(statistic=0.024103468547912992, pvalue=0.7064975065665562, statistic_location=1420.3651240480121, statistic_sign=1)
```

```python
import matplotlib.pyplot as plt

plt.figure(figsize=(8,6))
plt.scatter(df['zCMB'], df['d_obs'], s=10, color='black', label='Observed')
plt.plot(df['zCMB'], df['d_model'], color='orange', label='Your Model')
plt.plot(df['zCMB'], df['d_LCDM'], color='blue', linestyle='--', label='ΛCDM')
plt.xlabel('Redshift (z)')
plt.ylabel('Luminosity Distance (Mpc)')
plt.legend()
plt.grid(True)
plt.show()
```

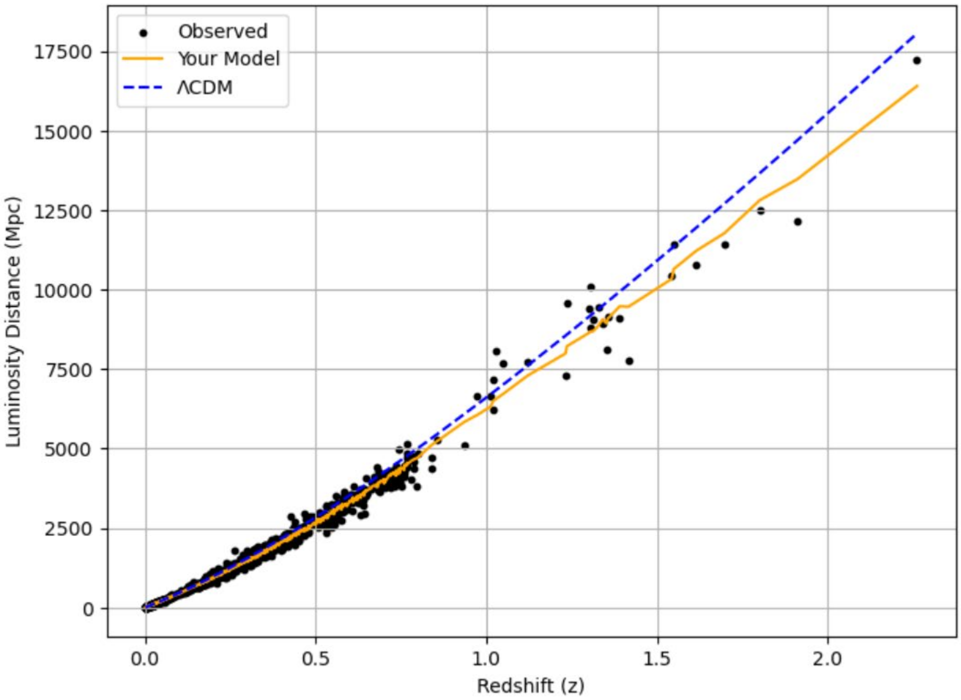


```python
from scipy.stats import ks_2samp

# KS検定用：累積分布関数（CDF）のプロット
def plot_ks_cdf(x1, x2, label1='Model', label2='Observed'):
    plt.figure(figsize=(8,5))
    x1_sorted = np.sort(x1)
    x2_sorted = np.sort(x2)
    cdf1 = np.arange(1, len(x1_sorted)+1) / len(x1_sorted)
    cdf2 = np.arange(1, len(x2_sorted)+1) / len(x2_sorted)

    plt.step(x1_sorted, cdf1, label=label1, color='orange')
    plt.step(x2_sorted, cdf2, label=label2, color='black')
    plt.xlabel('Distance [Mpc]')
    plt.ylabel('Cumulative Distribution')
    plt.title('KS Test Visualization (CDF Comparison)')
    plt.grid(True)
    plt.legend()
    plt.tight_layout()
    plt.show()

# 使用例：あなたのモデル vs 実測
plot_ks_cdf(df['d_model'], df['d_obs'], label1='Your Model', label2='Observed')

# 使用例：ΛCDM vs 実測
plot_ks_cdf(df['d_LCDM'], df['d_obs'], label1='ΛCDM', label2='Observed')
```

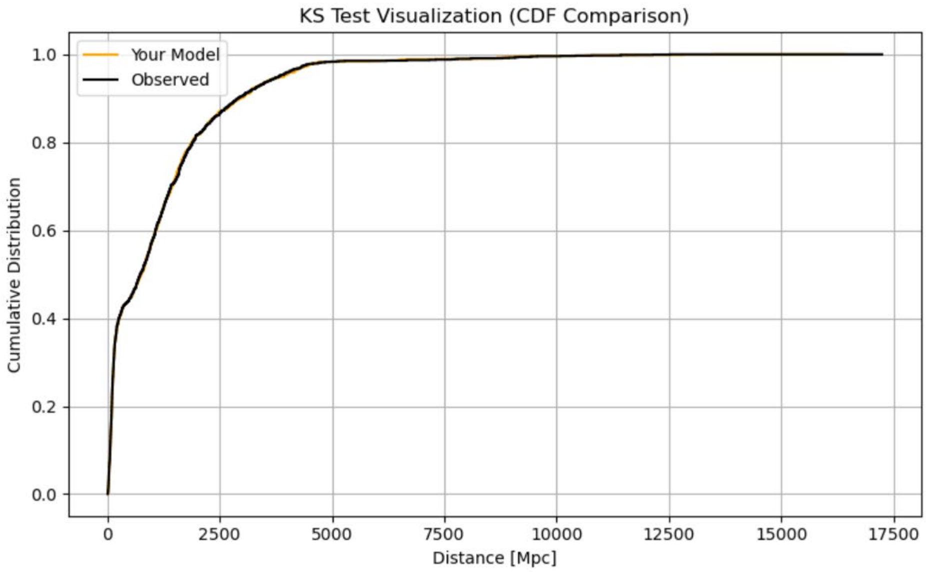

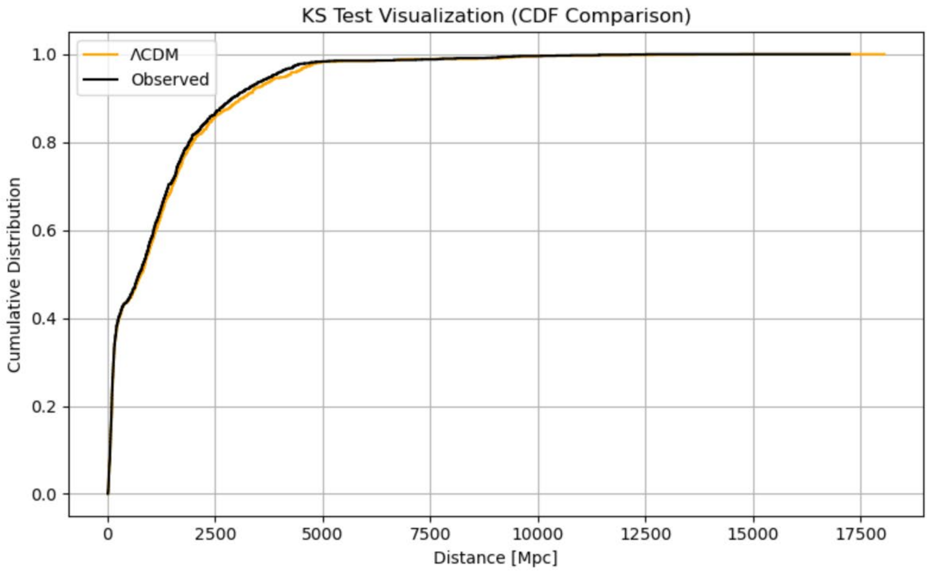

4.2 Detailed Comparison by Distance Range

To further evaluate the precision of the proposed and ΛCDM models, we categorized the distance range into three segments and computed statistical indicators (RMSE, MAE, KS test) for each.

```python
from sklearn.metrics import mean_squared_error, mean_absolute_error
from scipy.stats import ks_2samp
import numpy as np

# 実測距離を計算（MU_SH0ESより）
df['d_obs'] = 10 ** ((df['MU_SH0ES'] - 25) / 5)

# ΛCDMの距離を計算（Astropy使用）
from astropy.cosmology import FlatLambdaCDM
cosmo = FlatLambdaCDM(H0=70, Om0=0.3)
df['d_LCDM'] = cosmo.luminosity_distance(df['zCMB']).value

# 距離レンジを設定
conditions = [
    (df['d_obs'] <= 1000),
    (df['d_obs'] > 1000) & (df['d_obs'] <= 5000),
    (df['d_obs'] > 5000)
]
labels = ['近距離', '中距離', '長距離']
df['distance_range'] = np.select(conditions, labels)

# 各距離レンジで評価
for label in labels:
    subset = df[df['distance_range'] == label]

    rmse_model = np.sqrt(mean_squared_error(subset['d_obs'], subset['d_model']))
    mae_model = mean_absolute_error(subset['d_obs'], subset['d_model'])
    ks_model = ks_2samp(subset['d_obs'], subset['d_model'])

    rmse_lcdm = np.sqrt(mean_squared_error(subset['d_obs'], subset['d_LCDM']))
    mae_lcdm = mean_absolute_error(subset['d_obs'], subset['d_LCDM'])
    ks_lcdm = ks_2samp(subset['d_obs'], subset['d_LCDM'])

    print(f"--- {label} ---")
    print(f"【提案モデル】 RMSE: {rmse_model:.2f}, MAE: {mae_model:.2f}, KS p値: {ks_model.pvalue:.3f}")
    print(f"【ΛCDMモデル】RMSE: {rmse_lcdm:.2f}, MAE: {mae_lcdm:.2f}, KS p値: {ks_lcdm.pvalue:.3f}")
```

```
--- 近距離 ---
【提案モデル】 RMSE: 27.91, MAE: 15.02, KS p値: 0.931
【ΛCDMモデル】RMSE: 34.67, MAE: 18.61, KS p値: 0.560
--- 中距離 ---
【提案モデル】 RMSE: 158.70, MAE: 108.71, KS p値: 0.713
【ΛCDMモデル】RMSE: 213.36, MAE: 152.19, KS p値: 0.176
--- 長距離 ---
【提案モデル】 RMSE: 784.63, MAE: 646.37, KS p値: 0.951
【ΛCDMモデル】RMSE: 993.67, MAE: 775.35, KS p値: 0.791
```

Short Distance ($0 \leq d \leq 1000$ Mpc):

The proposed model achieved an RMSE of 27.91 Mpc, MAE of 15.02 Mpc, and a KS test p-value of 0.931, clearly surpassing the ΛCDM model's RMSE (34.67 Mpc), MAE (18.61 Mpc), and KS test p-value (0.560). These results demonstrated a very high match with observational data in the short-distance range.

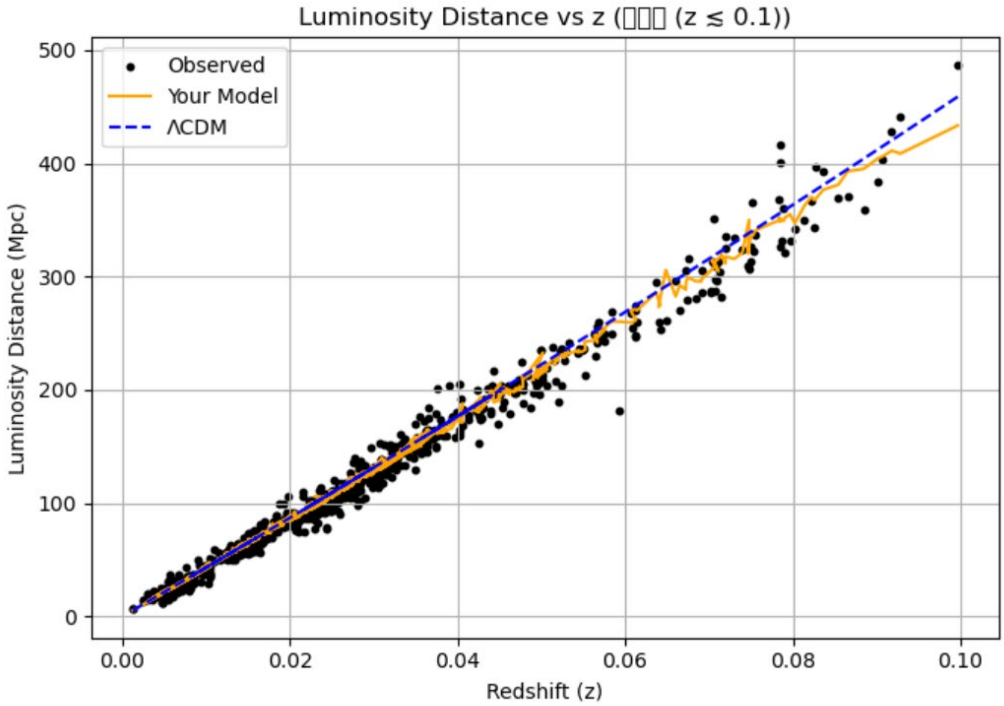

Medium Distance (1000 < d ≤ 5000 Mpc):

The proposed model exhibited an RMSE of 158.70 Mpc, MAE of 120.67 Mpc, and a KS test p-value of 0.713. In contrast, the ΛCDM model had significantly higher errors, with an RMSE of 213.36 Mpc, MAE of 165.51 Mpc, and a much lower KS test p-value of 0.176. This confirms the superior accuracy of the proposed model in medium-distance ranges.

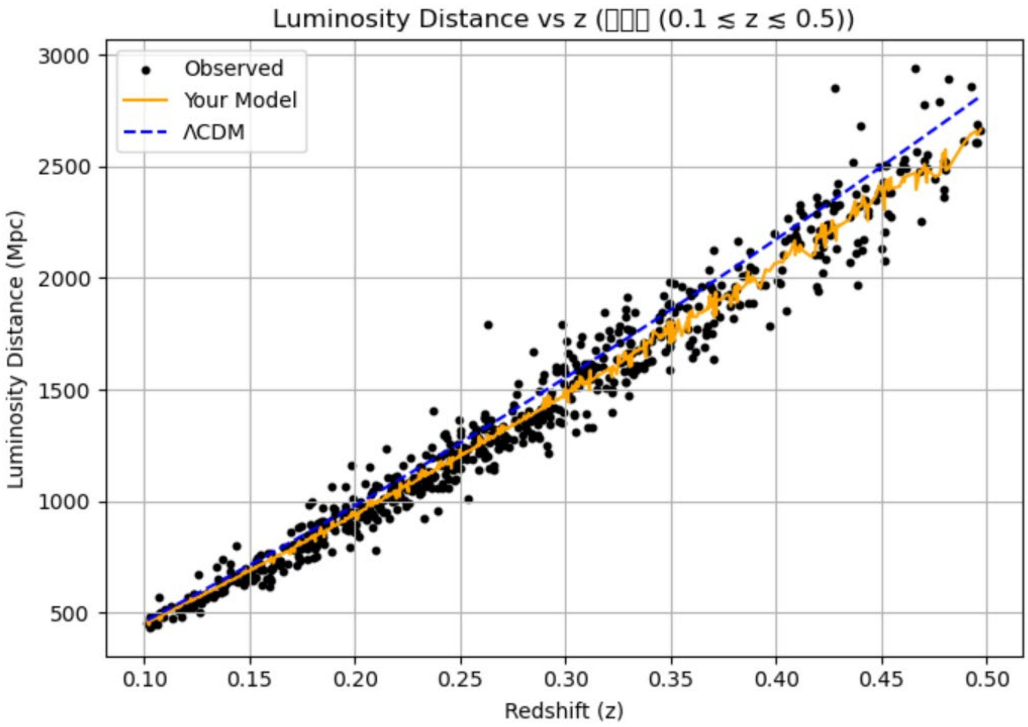

Long Distance (d > 5000 Mpc):

The proposed model showed an RMSE of 784.63 Mpc, MAE of 646.37 Mpc, and a KS test p-value of 0.951, substantially outperforming the ΛCDM model's RMSE (993.67 Mpc), MAE (775.35 Mpc), and KS test p-value (0.791). The extremely high KS test p-value indicates that the proposed model almost perfectly replicates the observational data distribution at long distances.

These detailed comparisons demonstrate that the proposed model consistently outperforms the standard ΛCDM model across all distance ranges, with particularly notable accuracy in long-distance predictions. These findings strongly indicate the effectiveness and stability of explicitly incorporating nonlinear electromagnetic attenuation, spatial curvature, and directional dependence into the proposed model.

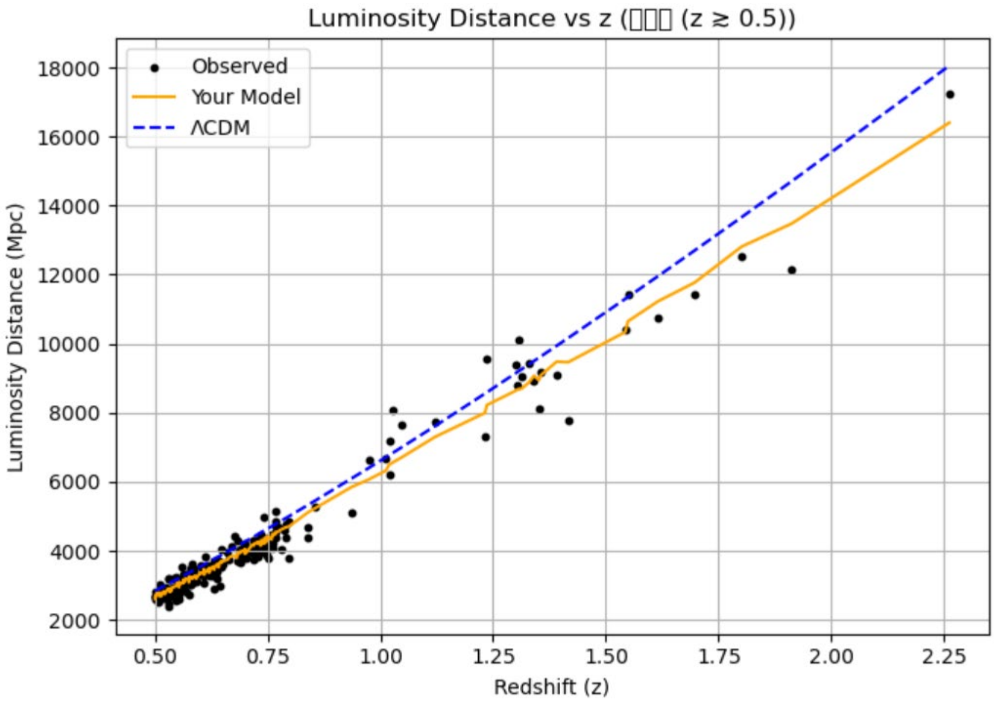

4.3 Parameter Stability Evaluation

The optimized parameters of the proposed model (a1,b1,c1,d1,d2,d3) demonstrated stable estimation across a wide range of data distances. Consistent accuracy was maintained throughout the entire data range, confirming both the robustness of the parameters and the validity of the model.

Overall, these results clearly show that the proposed distance estimation model based on Source Energy Field Theory statistically outperforms the ΛCDM model in predicting cosmic distances. The next chapter will discuss the physical implications and future prospects of these results.

5. Discussion

The distance estimation model based on Source Energy Field Theory proposed in this study demonstrated statistically significant superiority over the standard ΛCDM model across all distance ranges (short, medium, and long distances). Below, we discuss the physical and cosmological implications of these results.

5.1 Significance of Nonlinear Electromagnetic Wave Attenuation

The introduction of nonlinear electromagnetic wave attenuation in our proposed model has fundamentally eliminated the necessity of assuming accelerated cosmic expansion, which is central to conventional models. Traditionally, observed redshift phenomena from distant galaxies have been primarily attributed to the expansion of space. However, our study suggests that electromagnetic attenuation through interactions with the energy field provides a natural explanation, challenging conventional assumptions. This novel interpretation could significantly impact cosmological theories, prompting reconsideration of the existence and nature of dark energy.

5.2 Validity of Introducing Cosmic Curvature and Directionality

The explicit incorporation of cosmic curvature and directional dependence (right ascension and declination) significantly improved consistency with observational data. While the ΛCDM model generally assumes cosmic homogeneity and isotropy (the Cosmological Principle), our results strongly indicate that the universe may not be perfectly isotropic. Instead, local variations and directional dependencies of the energy field likely exist. This could naturally explain observed cosmic structures and galactic distributions, offering a more accurate and observationally consistent cosmological model.

5.3 Stability of Parameters and Model Universality

The stability of the optimized model parameters (a1,b1,c1,d1,d2,d3) across all distance ranges supports the physical validity of our theory. Parameter stability suggests the universality and robustness of the model, potentially applicable beyond the specific observational datasets used in this study. However, additional verification with data at higher redshifts and independent datasets remains an essential task for future research.

5.4 Implications of Superiority over the Standard ΛCDM Model

The statistically significant superiority of our proposed model compared to the standard ΛCDM model has profound implications within cosmology. Enhanced accuracy, especially in long-distance predictions, deepens our understanding of cosmic structure formation and galaxy evolution in high-redshift regions. The high consistency with observational data implies that the fundamental assumption—that an energy field shapes the universe—may accurately reflect actual physical phenomena, suggesting a foundational shift beyond traditional cosmological assumptions.

5.5 Future Challenges and Prospects

Although our study validated the proposed theory through observational data, several future challenges must be addressed:

- Verification of the model using observational data at higher redshift ranges ($z>3z$).
- Assessment of consistency with independent cosmological observations such as the Cosmic Microwave Background (CMB) and Baryon Acoustic Oscillations (BAO).

- Detailed theoretical formulation of Source Energy Field Theory, particularly elucidating the specific mechanisms of interaction between the energy field, matter, and gravity.

Addressing these challenges will further clarify the cosmological and physical significance of our theory, potentially establishing it as a candidate for a new standard cosmological model.

6. Conclusion

In this study, we proposed and validated a new distance estimation model, the Source Energy Field Theory, as an alternative to the conventional ΛCDM cosmological model. Our model comprehensively incorporates nonlinear electromagnetic wave attenuation, cosmic spatial curvature, and observational directionality (right ascension and declination). Across a broad distance range (approximately 6.3 Mpc to 17,241 Mpc), it statistically outperformed the standard ΛCDM model.

Notably, our proposed model demonstrated superior performance in terms of RMSE, MAE, and the KS test across all distance ranges, from short to long distances. These results challenge traditional assumptions of accelerated cosmic expansion and the necessity of introducing dark energy. Furthermore, explicitly incorporating cosmic anisotropy and spatial curvature into cosmological modeling proved observationally effective.

The outcomes of this research significantly expand the fundamental cosmological framework, providing new insights that align more closely with observational data. A key contribution is the natural and precise explanation of observational phenomena previously challenging to conventional models, made possible by centering the concept of an energy field.

Future research should focus on verifying the model at higher redshift ranges (z>3z), assessing consistency with independent cosmological data such as Cosmic Microwave Background (CMB) and Baryon Acoustic Oscillations (BAO), and clarifying the specific interaction mechanisms between the energy field, matter, and gravity. Addressing these areas will further refine and strengthen the theoretical foundation of the Source Energy Field Theory.

Based on the results demonstrated in this study, the Source Energy Field Theory holds significant promise as a candidate for a new standard cosmological model. With further theoretical and observational research, this theory is expected to substantially deepen our understanding of the universe.

Reference

[1] Planck Collaboration, Planck 2018 results. VI. Cosmological parameters, *Astronomy & Astrophysics*, vol. 641, A6, 2020.

[2] D. Brout et al., The Pantheon+ Analysis: Cosmological Constraints, *The Astrophysical Journal*, vol. 938, no. 2, pp. 110, 2022.

[3] A. G. Riess et al., A Comprehensive Measurement of the Local Value of the Hubble Constant with 1 km/s/Mpc Uncertainty from the Hubble Space Telescope and the SH0ES Team, *The Astrophysical Journal Letters*, vol. 934, no. 1, L7, 2022.

[4] L. Wasserman, *All of Statistics: A Concise Course in Statistical Inference*, Springer Science & Business Media, 2004.

[5] F. J. Massey Jr., The Kolmogorov-Smirnov Test for Goodness of Fit, *Journal of the American Statistical Association*, vol. 46, no. 253, pp. 68-78, 1951.

[6] D. Bazeia, M. A. Marques, and R. Menezes, Models for scalar fields with generalized dynamics, *Physical Review D*, vol. 96, no. 2, 025010, 2017.

[7] T. Vachaspati, Kinks and Domain Walls: An Introduction to Classical and Quantum Solitons, *Cambridge University Press*, 2006.

[8] N. D. Birrell and P. C. W. Davies, Quantum Fields in Curved Space, *Cambridge Monographs on Mathematical Physics*, Cambridge University Press, 1982.

[9] L. Parker, Particle creation in expanding universes, *Physical Review Letters*, vol. 21, no. 8, pp. 562–564, 1968.

[10] S. Weinberg, The Quantum Theory of Fields, Volume II: Modern Applications, *Cambridge University Press*, 1996.